

## Reconstruction of the projected crystal potential in high-resolution transmission electron microscopy

M. Lentzen<sup>1</sup>

1. Institute of Solid State Research and Ernst Ruska Centre for Microscopy, Research Centre Jülich, 52425 Jülich, Germany

m.lentzen@fz-juelich.de

Keywords: potential reconstruction, high-resolution electron microscopy, sub-angstrom resolution, phenomenological absorption

In high-resolution transmission electron microscopy information on the object under investigation can be derived from recorded image intensities or, by means of wave function reconstruction [1–3], from exit wave functions. The recorded image intensities, however, are affected in all practical cases by non-linear imaging artifacts and by lens aberrations of the instrument, which induce unwanted contrast delocalisation [4]; both may obscure structural detail. Even after wave function reconstruction, which improves the conditions for structural investigations, information on the local atomic arrangement is obscured by dynamical electron scattering, which leads to a non-linear relation between scattering power and modulation of the exit wave function.

The reconstruction of the projected crystal potential from a measured exit wave function would remove the unwanted effects of dynamical electron scattering on the imaging of atomic structures and thus allow direct structural measurements and interpretation.

It was therefore a long-standing aim to find a reliable reconstruction algorithm [5, 6], but only through the strict wave-mechanical treatment by Lentzen and Urban [7] a rapid and stable algorithm could be derived. Together with the use of the channelling model of electron diffraction [8, 9] a successful reconstruction of the crystal potential was achieved for non-periodic objects over a wide thickness range. In order to use the potential reconstruction algorithm [7] in real materials science investigations still a few theoretical and practical problems had to be considered. The most demanding problem was the inclusion of phenomenological absorption, which distinctly alters the modulation of an exit wave already for objects of a few nanometres in thickness.

The core of the new potential reconstruction algorithm is the refinement  $\delta U(\mathbf{r})$  of the projected potential  $U(\mathbf{r})$ , with  $\psi_e(\mathbf{r}, t')$  the difference of the experimental and the simulated exit wave being back-propagated through the object from the exit plane  $t$  to a plane  $t'$  inside the crystal,  $\psi_s(\mathbf{r}, t')$  the entrance plane wave being propagated through the object to the same plane  $t'$  inside the crystal,  $\lambda$  the electron wavelength, and  $\kappa$  the phenomenological absorption:

$$\delta U(\mathbf{r}) = \frac{2}{\pi\lambda t^2} \operatorname{Im} \left\{ (1 - i\kappa) \int_0^t \psi_s^*(\mathbf{r}, t') \psi_e(\mathbf{r}, t') dt' \right\}.$$

The reconstruction is successful regardless of the scattering power even for the case of strong dynamical electron scattering [10]. A simulation study assuming an  $\text{YBa}_2\text{Cu}_3\text{O}_7$  crystal in [100] orientation of 3.8 nm in thickness, an absorption of 0.2, leading to an intensity loss of 22% at an accelerating voltage of 200 kV, and an instrumental information limit of 0.05 nm shows that the projected crystal potential can be measured with an r.m.s. accuracy of better than 2%. Real part, imaginary part, amplitude, and phase of the exit wave function displayed in Figure 1 show that dynamical diffraction prevails, in particular through

both the phase wrap and the negative value of the imaginary part at the Ba positions. The reconstructed potential displayed in Figure 2 shows, in contrast to the various views of the exit wave function, that apart from the high reconstruction accuracy a direct structure interpretation is possible with respect to weakly scattering O atom columns, the Cu and Cu–O columns of medium scattering power, and the Y and Ba columns of strong scattering power.

A series of potential reconstructions with varying instrumental information limit, present in the exit wave function, shows further that for future instruments with sub-angstrom information limits of around 0.05 nm, see the table in Figure 2, a high measurement accuracy will open excellent prospects for quantitative materials science investigations.

1. H. Lichte, *Ultramicroscopy* **20** (1986) p293.
2. W. Coene et al., *Phys. Rev. Lett.* **69** (1992) p3743.
3. A. Thust et al., *Ultramicroscopy* **64** (1996) p211.
4. W. Coene and A.J.E.M. Jansen, *Scan. Microsc. Suppl.* **6** (1992) p379.
5. M.A. Gribelyuk, *Acta Cryst.* **A47** (1991) p715.
6. M.J. Beeching and A.E.C. Spargo, *Ultramicroscopy* **52** (1993) p243.
7. M. Lentzen and K. Urban, *Acta Cryst.* **A56** (2000) p235.
8. K. Kambe et al., *Z. Naturforsch.* **A29** (1974) p1034.
9. F. Fujimoto, *Phys. Status Solidi* **A45** (1978) p99.
10. M. Lentzen and K. Urban, *EMC 2008* **1** (2008) p131.

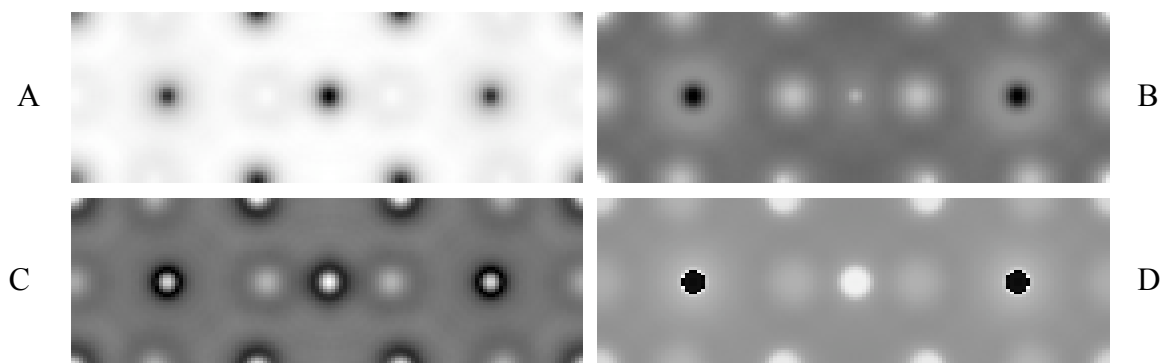


**Figure 1.** Exit wave function of  $\text{YBa}_2\text{Cu}_3\text{O}_7$  [100] at an accelerating voltage of 200 kV, a thickness of 3.8 nm, and an absorption of 0.2; (A) real part; (B) imaginary part; (C) amplitude; (D) phase. The unit cell measures 1.1683 nm  $\times$  0.3887 nm.

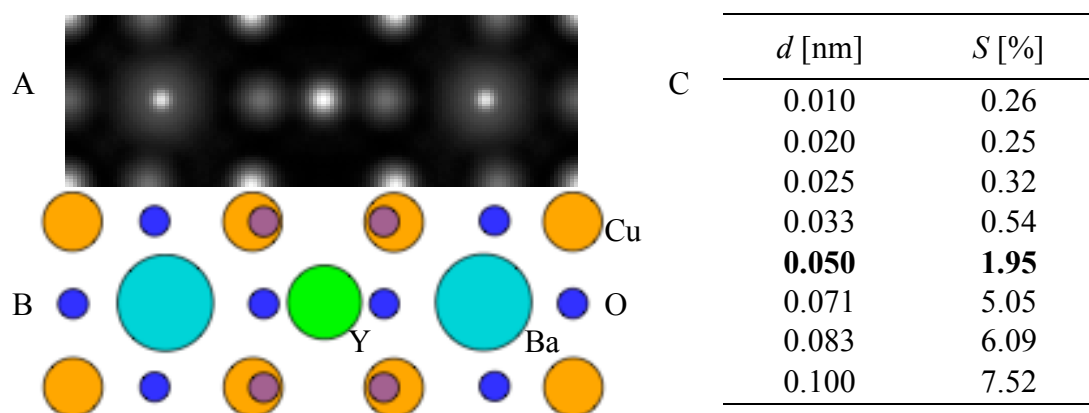


**Figure 2.** (A) Projected crystal potential reconstructed from the exit wave function displayed in Figure 1. (B) Atomic model of the  $\text{YBa}_2\text{Cu}_3\text{O}_7$  [100] unit cell. (C) Instrumental information limit  $d$  and r.m.s. reconstruction accuracy  $S$  after 60 refinement steps.